



Contents lists available at SciVerse ScienceDirect

# Spectrochimica Acta Part A: Molecular and Biomolecular Spectroscopy

journal homepage: [www.elsevier.com/locate/saa](http://www.elsevier.com/locate/saa)

## Vibrational spectroscopic investigations and computational study of 5-*tert*-Butyl-*N*-(4-trifluoromethylphenyl)pyrazine-2-carboxamide



Tomy Joseph<sup>a,d</sup>, Hema Tresa Varghese<sup>b</sup>, C. Yohannan Panicker<sup>c,\*</sup>, K. Viswanathan<sup>d</sup>, Martin Dolezal<sup>e</sup>, T.K. Manojkumar<sup>f</sup>, Christian Van Alsenoy<sup>g</sup>

<sup>a</sup> Department of Physics, St. Xavier's College, Vaikom, Kothavara, Kottayam, Kerala, India

<sup>b</sup> Department of Physics, Fatima Mata National College, Kollam, Kerala, India

<sup>c</sup> Department of Physics, TKM College of Arts and Science, Kollam, Kerala, India

<sup>d</sup> Department of Physics, Karpagam University, Pollachi Main Road, Eachanari, Coimbatore, Tamilnadu, India

<sup>e</sup> Faculty of Pharmacy in Hradec Kralove, Charles University in Prague, Heyrovskeho 1203, Hradec Kralove 500 05, Czech Republic

<sup>f</sup> Indian Institute of Information Technology and Management – Kerala, Technopark Campus, Trivandrum, Kerala, India

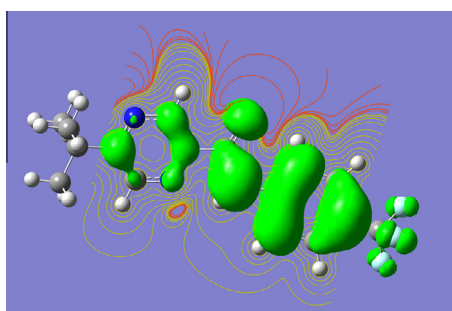
<sup>g</sup> Department of Chemistry, University of Antwerp, B2610 Antwerp, Belgium

### H I G H L I G H T S

- IR, Raman and NBO were reported.
- The wavenumbers are calculated theoretically using Gaussian09 software.
- The wavenumbers are assigned using PED analysis.
- The geometrical parameters are in agreement with that of similar derivatives.

### G R A P H I C A L A B S T R A C T

Quantum chemical calculations of the equilibrium geometry, harmonic vibrational frequencies, infrared intensities and Raman activities of 5-*tert*-Butyl-*N*-(4-trifluoromethylphenyl)pyrazine-2-carboxamide in the ground state were carried out by using density functional methods. Potential energy distribution of normal modes of vibrations was done using GAR2PED program. Nonlinear optical behavior of the examined molecule was investigated by the determination of first hyperpolarizability. The calculated HOMO and LUMO energies show the chemical activity of the molecule. The stability of the molecule arising from hyper-conjugative interaction and charge delocalization has been analyzed using NBO analysis. The calculated geometrical parameters are in agreement with that of similar derivatives. The stability of the molecule arising from hyper-conjugative interaction and charge delocalization has been analyzed using NBO analysis.



### A R T I C L E I N F O

#### Article history:

Received 6 January 2013

Received in revised form 14 April 2013

Accepted 24 April 2013

Available online 6 May 2013

#### Keywords:

FT-IR

FT-Raman

### A B S T R A C T

Pyrazine and its derivatives form an important class of compounds present in several natural flavors and complex organic molecules. Quantum chemical calculations of the equilibrium geometry, harmonic vibrational frequencies, infrared intensities and Raman activities of 5-*tert*-Butyl-*N*-(4-trifluoromethylphenyl)pyrazine-2-carboxamide in the ground state were carried out by using density functional methods. Potential energy distribution of normal modes of vibrations was done using GAR2PED program. Nonlinear optical behavior of the examined molecule was investigated by the determination of first hyperpolarizability. The calculated HOMO and LUMO energies show the chemical activity of the molecule. The stability of the molecule arising from hyper-conjugative interaction and charge delocalization

\* Corresponding author. Tel.: +91 9895370968.

E-mail address: [cyphyp@rediffmail.com](mailto:cyphyp@rediffmail.com) (C. Yohannan Panicker).

Pyrazine  
Carboxamide  
PED

has been analyzed using NBO analysis. The calculated geometrical parameters are in agreement with that of similar derivatives. The stability of the molecule arising from hyper-conjugative interaction and charge delocalization has been analyzed using NBO analysis.

© 2013 Elsevier B.V. All rights reserved.

## Introduction

Pyrazine and its derivatives form an important class of compounds present in several natural flavors and complex organic molecules [1]. 2-Chloropyrazine and 2,6-dichloropyrazine are mainly found as medical and agricultural drug intermediates [1–3]. Pyrazine derivatives are important drugs with antibacterial, diuretic, hypolipidemic, antidiabetic, hypnotic, anticancer and antiviral activity. Pyrazinamide (PZA), another first-line TB drug, was discovered through an effort to find antitubercular nicotinamide derivatives [4]. The activity of PZA appears to be pH dependent, since it is bactericidal at pH 5.5, but inactive at neutral pH. PZA is used in combinations with INH and rifampicin. It is especially effective against semi-dormant mycobacteria. Its mechanism of action appears to involve its hydrolysis to pyrazinoic acid via the bacterial enzyme *pmcA* [5]. PZA can also be metabolized by hepatic microsomal deamidase to pyrazinoic acid, which is a substrate for xanthine oxidase, affording 5-hydroxypyrazinoic acid. The acid is believed to act as an anti-metabolite of nicotinamide and interferes with NAD biosynthesis. A different analog of PZA, 5-chloropyrazine-2-carboxamide, has previously been shown to inhibit mycobacterial fatty acid synthase I [6]. Pyrazinamide is a member of the pyrazine family and it is known as a very effective antimycobacterial agent, with a well established role in tuberculosis treatment [7]. Pyrazinamide is bactericidal to semidormant mycobacteria and reduces total treatment time [8]. Although the exact biochemical basis of pyrazinamide activity *in vivo* is not known, under acidic conditions it is thought to be a prodrug of pyrazinoic acid, a compound with antimycobacterial activity [9]. The finding that pyrazinamide-resistant strains lose amidase (pyrazinamidase or nicotinamidase) activity and the hypothesis that amidase is required to convert pyrazinamide to pyrazinoic acid intracellularly led to the recent synthesis and study of various prodrugs of pyrazinoic acid [10]. The resistance of PZA arises by the absence of the enzyme, *Pmc A*. The major side effect of PZA is dose-related hepatotoxicity. Pyrazinoic acid disrupts membrane energetics and inhibits membrane transport function in *M.tuberculosis* [11]. The dynamical pattern of the 2-amino-pyrazine-3-carboxylic acid molecule by inelastic and incoherent neutron scattering, Raman spectroscopy and *ab initio* calculations was reported by Pawlukojc et al. [12]. Billes et al. [13] calculated the vibrational frequencies of the three parent diazines (pyrazine, pyridazine and pyrimidine) applying *ab initio* quantum chemical methods, Moller-Pleassett perturbation and local density function methods. Various compounds possessing –NHCO– groups, e.g. substituted amides, acyl and thioacyl anilides, benzanilides, phenyl carbamates, etc., were found to inhibit photo synthetic electron transport [14,15]. Therefore, the vibrational spectroscopic studies of the amides of pyrazine-2-carboxylic acids are added areas of interest. In the present work, FT-IR and FT-Raman spectra of 5-*tert*-Butyl-*N*-(4-trifluoromethylphenyl)pyrazine-2-carboxamide are reported both experimentally and theoretically. The HOMO and LUMO analysis have been used to elucidate information regarding charge transfer within the molecule. The stability of the molecule arising from hyper-conjugative interaction and charge delocalization has been also analyzed using NBO analysis.

## Experimental

All organic solvents used for the synthesis were of analytical grade. The solvents were dried and freshly distilled under argon atmospheres. Melting point was determined using a SMP 3 melting point apparatus (BIBBYB Stuart Scientific, UK) and are uncorrected. The reactions were monitored and the purity was checked by TLC (Merck UV 254 TLC plates, Darmstadt, Germany) using petroleum ether/EtOAc (9:1) as developing solvent. Purification of compounds was made using Flash Master Personal chromatography system from Argonaut Chromatography (Argonaut Technologies, Redwood City, CA, USA) with gradient of elution from 0% to 20% ethyl-acetate in hexane. As sorbent, Merck Silica Gel 60 (0.040–0.063 mm) was used (Merck). Elemental analysis was performed on an automatic microanalyser CHNS-O CE instrument (FISONS EA 1110, Milano, Italy). <sup>1</sup>H- and <sup>13</sup>C-NMR spectra were recorded (at 300 MHz for <sup>1</sup>H and 75 MHz for <sup>13</sup>C) in CDCl<sub>3</sub> solutions at ambient temperature on a Varian Mercury-Vx BB 300 instrument (Varian, Palo Alto, CA, USA). The chemical shifts were recorded as  $\delta$  values in ppm and were indirectly referenced to tetramethylsilane (TMS) via the solvent signal (7.26 for <sup>1</sup>H and 77.0 for <sup>13</sup>C in CDCl<sub>3</sub>).

The 5-*tert*-butylpyrazine-2-carboxylic acid [16] (50.0 mmol) and thionyl chloride (5.5 mL, 75.0 mmol) in dry toluene (20 mL) was refluxed for about 1 h. Excess thionyl chloride was removed by repeated evaporation with dry toluene *in vacuo*. The crude acyl chloride dissolved in dry acetone (50 mL) was added drop wise to a stirred solution of the 4-trifluoromethylaniline (50.0 mmol) and pyridine (50.0 mmol) in dry acetone (50 mL) kept at room temperature. After the addition was complete, stirring was continued for 30 min, then the reaction mixture was poured into cold water (100 mL) and the crude amide was collected and purified by the column chromatography.

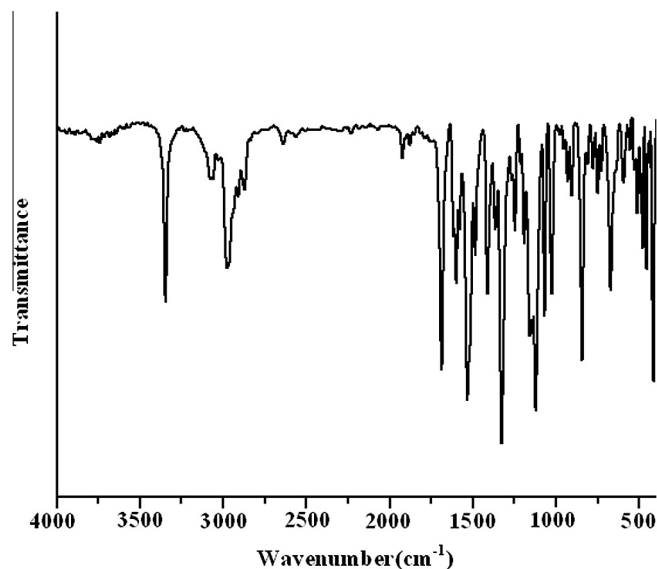
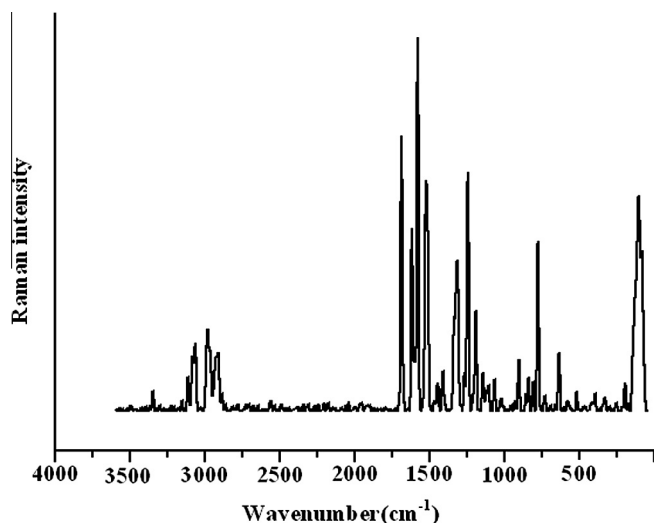


Fig. 1. FT-IR spectrum of 5-*tert*-Butyl-*N*-(4-trifluoromethylphenyl)pyrazine-2-carboxamide.



**Fig. 2.** FT-Raman spectrum of 5-*tert*-Butyl-*N*-(4-trifluoromethylphenyl)pyrazine-2-carboxamide.

5-*tert*-Butyl-*N*-(4-trifluoromethylphenyl)pyrazine-2-carboxamide. Yield 57%; Anal. Calcd. for  $C_{16}H_{16}F_3N_3O$  (323.3): 59.44% C, 4.99% H, 13.00% N; Found: 59.54% C, 3.97% H, 12.94% N; M.p. 117.2–118.0 °C; Log *P*: 3.64; Clog *P*: 4.22870;  $^1H$ -NMR ( $CDCl_3$ )  $\delta$ : 9.81 (1H, bs, 20H), 9.40 (1H, d,  $J = 1.5$  Hz, 7H), 8.64 (1H, d,  $J = 1.5$  Hz, 26H), 7.93–7.85 (2H, m, AA', BB', 16H, 17H), 7.69–7.61 (2H, m, AA', BB', 15H, 21H), and 1.45 (9H, s, 31H, 32H, 33H, 34H, 35H, 36H, 37H, 38H, 39H).  $^{13}C$ -NMR ( $CDCl_3$ )  $\delta$ : 165.1, 160.1, 145.9, 140.6, 140.4, 140.1, 126.4 (q,  $J = 3.8$  Hz), 126.0 (q,  $J = 32.7$  Hz), 124.0 (q,  $J = 271.7$  Hz), 119.5, 39.1, and 28.2 [17].

The FT-IR spectrum (Fig. 1) was recorded using KBr pellets on a DR/Jasco FT-IR 6300 spectrometer in KBr pellets. The spectral resolution was  $2\text{ cm}^{-1}$ . The FT-Raman spectrum (Fig. 2) was obtained on a Bruker RFS 100/s, Germany. For excitation of the spectrum the emission of Nd:YAG laser was used, excitation wavelength 1064 nm, maximal power 150 mW, measurement on solid sample. The spectral resolution after apodization was  $2\text{ cm}^{-1}$ .

### Computational details

Calculations of the title compound were carried out with Gaussian09 software [18] program using B3LYP/6-31G\*,

B3PW91/6-31G\* and B3LYP/SDD basis sets to predict the molecular structure and vibrational wavenumbers. Calculations were carried out with Becke's three parameter hybrid model using the Lee–Yang–Parr correlation functional (B3LYP) method. Molecular geometries were fully optimized by Berny's optimization algorithm using redundant internal coordinates. Harmonic vibrational wavenumbers were calculated using analytic second derivatives to confirm the convergence to minima on the potential surface. The Stuttgart/Dresden effective core potential basis set (SDD) [19] was chosen particularly because of its advantage of using faster calculations with relatively better accuracy and structures [20]. Then frequency calculations were employed to confirm the structure as minimum points in energy. At the optimized structure (Fig. 3) of the examined species, no imaginary wavenumber modes were obtained, proving that a true minimum on the potential surface was found. The DFT method tends to over estimate the fundamental modes; therefore scaling factor (0.9613) has to be used for obtaining a considerably better agreement with experimental data [21]. The observed disagreement between theory and experiment could be a consequence of the anharmonicity and of the general tendency of the quantum chemical methods to over estimate the force constants at the exact equilibrium geometry. The optimized geometrical parameters (B3LYP/SDD) are given in table 1. The assignments of the calculated wavenumbers are aided by the animation option of GAUSSVIEW program, which gives a visual presentation of the vibrational modes [22]. The potential energy distribution (PED) is calculated with the help of GAR2PED software package [23].

### Results and discussion

#### IR and Raman spectra

The observed IR, Raman bands and calculated wavenumbers (scaled) and assignments are given in table 2. The C=O stretching vibrations are expected in the range  $1715\text{--}1600\text{ cm}^{-1}$  and the deformation modes of C=O in the range  $460\text{--}800\text{ cm}^{-1}$  [24]. In the case of 2-aminopyrazine-3-carboxylic acid [12] the C=O modes are reported as follows: torsional C=O 101 (Raman), 111 (HF); rocking C=O 537 (Raman), 571 (HF); wagging C=O 723 (Raman), 736 (HF); bending C=O 912 (Raman), 886 (HF) and stretching mode C=O 1718 (Raman),  $1786\text{ cm}^{-1}$  (HF). For the title compound, the C=O modes are observed at 1613,  $538\text{ cm}^{-1}$  in the IR spectrum, 1617, 698,  $115\text{ cm}^{-1}$  in the Raman spectrum and at 1610, 870, 708,  $557, 122\text{ cm}^{-1}$  theoretically (SDD).

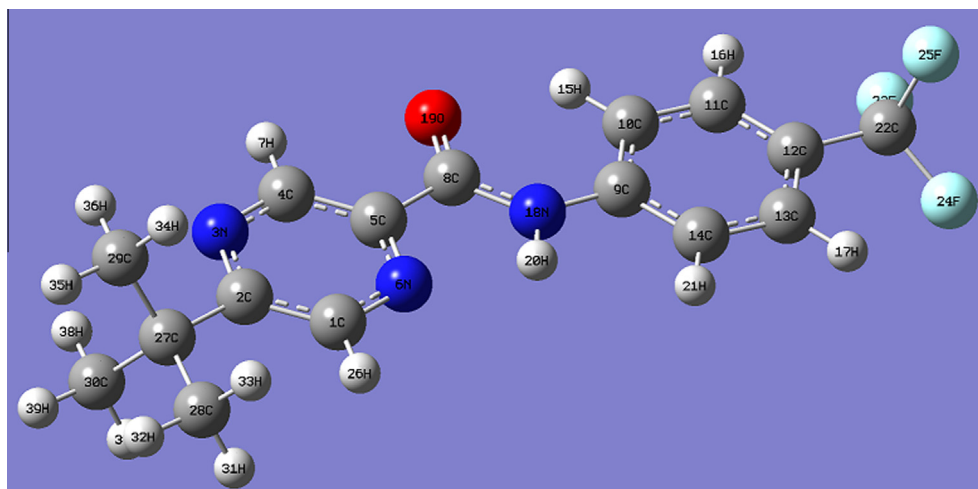


**Fig. 3.** Optimized geometry (SDD) of 5-*tert*-Butyl-*N*-(4-trifluoromethylphenyl) pyrazine-2-carboxamide.

**Table 1**  
Optimized geometrical parameters (SDD) of 5-*tert*-Butyl-*N*-(4-trifluoromethylphenyl)pyrazine-2-carboxamide, atom labeling according Fig. 3.

Bondlengths (Å)		Bondangles (°)		Dihedralangles (°)	
C <sub>1</sub> —C <sub>2</sub>	1.4185	A(2,1,6)	122.0	D(6,1,2,3)	−0.0
C <sub>1</sub> —N <sub>6</sub>	1.3522	A(2,1,26)	121.6	D(6,1,2,27)	180.0
C <sub>1</sub> —H <sub>26</sub>	1.0823	A(6,1,26)	116.4	D(26,1,2,3)	180.0
C <sub>2</sub> —N <sub>3</sub>	1.3670	A(1,2,3)	119.3	D(26,1,2,27)	−0.0
C <sub>2</sub> —C <sub>27</sub>	1.5326	A(1,2,27)	124.3	D(2,1,6,5)	−0.0
N <sub>3</sub> —C <sub>4</sub>	1.3509	A(3,2,27)	116.5	D(26,1,6,5)	180.0
C <sub>4</sub> —C <sub>5</sub>	1.4097	A(2,3,4)	118.8	D(1,2,3,4)	0.0
C <sub>4</sub> —H <sub>7</sub>	1.0839	A(3,4,5)	121.3	D(27,2,3,4)	−180.0
C <sub>5</sub> —N <sub>6</sub>	1.3581	A(3,4,7)	118.3	D(1,2,27,28)	−0.2
C <sub>5</sub> —C <sub>8</sub>	1.5050	A(5,4,7)	120.5	D(1,2,27,29)	120.7
C <sub>8</sub> —N <sub>18</sub>	1.3797	A(4,5,6)	120.7	D(1,2,27,30)	−121.1
C <sub>8</sub> —O <sub>19</sub>	1.2586	A(4,5,8)	121.1	D(3,2,27,28)	179.8
C <sub>9</sub> —C <sub>10</sub>	1.4165	A(6,5,8)	118.2	D(3,2,27,29)	−59.3
C <sub>9</sub> —C <sub>14</sub>	1.4168	A(1,6,5)	118.0	D(3,2,27,30)	58.9
C <sub>9</sub> —N <sub>18</sub>	1.4109	A(5,8,18)	112.8	D(2,3,4,5)	−0.0
C <sub>10</sub> —C <sub>11</sub>	1.4016	A(5,8,19)	121.4	D(2,3,4,7)	180.0
C <sub>10</sub> —H <sub>15</sub>	1.0819	A(18,8,19)	125.9	D(3,4,5,6)	−0.0
C <sub>11</sub> —C <sub>12</sub>	1.4079	A(10,9,14)	119.6	D(3,4,5,8)	180.0
C <sub>11</sub> —H <sub>16</sub>	1.0859	A(10,9,18)	123.0	D(7,4,5,6)	180.0
C <sub>12</sub> —C <sub>13</sub>	1.4091	A(14,9,18)	117.4	D(7,4,5,8)	−0.0
C <sub>12</sub> —C <sub>22</sub>	1.4951	A(9,10,11)	119.5	D(4,5,6,1)	0.0
C <sub>13</sub> —C <sub>14</sub>	1.3982	A(9,10,15)	119.6	D(8,5,6,1)	−180.0
C <sub>13</sub> —H <sub>17</sub>	1.0855	A(11,10,15)	120.9	D(4,5,8,18)	179.9
C <sub>14</sub> —H <sub>21</sub>	1.0877	A(10,11,12)	120.6	D(4,5,8,19)	−0.1
N <sub>18</sub> —H <sub>20</sub>	1.0210	A(10,11,16)	119.4	D(6,5,8,18)	−0.1
C <sub>22</sub> —F <sub>23</sub>	1.4042	A(12,11,16)	120.0	D(6,5,8,19)	179.9
C <sub>22</sub> —F <sub>24</sub>	1.4057	A(11,12,13)	120.0	D(5,8,18,9)	180.0
C <sub>22</sub> —F <sub>25</sub>	1.4168	A(11,12,22)	120.2	D(5,8,18,20)	−0.0
C <sub>27</sub> —C <sub>28</sub>	1.5476	A(13,12,22)	119.9	D(19,8,18,9)	−0.0
C <sub>27</sub> —C <sub>29</sub>	1.5570	A(12,13,14)	119.8	D(19,8,18,20)	180.0
C <sub>27</sub> —C <sub>30</sub>	1.5570	A(12,13,17)	120.2	D(14,9,10,11)	−0.2
C <sub>28</sub> —H <sub>31</sub>	1.0983	A(14,13,17)	120.0	D(14,9,10,15)	179.8
C <sub>28</sub> —H <sub>32</sub>	1.0966	A(9,14,13)	120.5	D(18,9,10,11)	−180.0
C <sub>28</sub> —H <sub>33</sub>	1.0983	A(9,14,21)	119.8	D(18,9,10,15)	−0.0
C <sub>29</sub> —H <sub>34</sub>	1.0983	A(13,14,21)	119.7	D(10,9,14,13)	0.2
C <sub>29</sub> —H <sub>35</sub>	1.0974	A(8,18,9)	128.6	D(10,9,14,21)	−179.7
C <sub>29</sub> —H <sub>36</sub>	1.0946	A(8,18,20)	113.3	D(18,9,14,13)	−180.0
C <sub>30</sub> —H <sub>37</sub>	1.0983	A(9,18,20)	118.1	D(18,9,14,21)	0.1
C <sub>30</sub> —H <sub>38</sub>	1.0946	A(12,22,23)	113.0	D(10,9,18,8)	−0.2
C <sub>30</sub> —H <sub>39</sub>	1.0974	A(12,22,24)	112.8	D(10,9,18,20)	179.8
		A(12,22,25)	113.2	D(14,9,18,8)	−180.0
		A(23,22,24)	106.7	D(14,9,18,20)	−0.0
		A(23,22,25)	105.3	D(9,10,11,12)	0.2
		A(24,22,25)	105.2	D(9,10,11,16)	179.6
		A(2,27,28)	112.3	D(15,10,11,12)	−179.8
		A(2,27,29)	108.2	D(15,10,11,16)	−0.4
		A(2,27,30)	108.2	D(10,11,12,13)	−0.2
		A(28,27,29)	109.4	D(10,11,12,22)	−177.9
		A(28,27,30)	109.4	D(16,11,12,13)	−179.6
		A(29,27,30)	109.2	D(16,11,12,22)	2.7
		A(27,28,31)	112.0	D(11,12,13,14)	0.2
		A(27,28,32)	109.2	D(11,12,13,17)	179.5
		A(27,28,33)	112.0	D(22,12,13,14)	177.9
		A(31,28,32)	107.4	D(22,12,13,17)	−2.8
		A(31,28,33)	108.6	D(11,12,22,23)	−31.8
		A(32,28,33)	107.4	D(11,12,22,24)	−152.9
		A(27,29,34)	111.3	D(11,12,22,25)	87.7
		A(27,29,35)	109.8	D(13,12,22,23)	150.5
		A(27,29,36)	110.5	D(13,12,22,24)	29.4
		A(34,29,35)	108.1	D(13,12,22,25)	−90.0
		A(34,29,36)	108.4D(12,13,14,9)	−0.2	
		A(35,29,36)	108.7	D(12,13,14,21)	179.7
		A(27,30,37)	111.3	D(17,13,14,9)	−179.6
		A(27,30,38)	110.5	D(17,13,14,21)	0.4
		A(27,30,39)	109.8	D(2,27,28,31)	−61.1
		A(37,30,38)	108.4	D(2,27,28,32)	−180.0
		A(37,30,39)	108.1	D(2,27,28,33)	61.2
		A(38,30,39)	108.7	D(29,27,28,31)	178.7
				D(29,27,28,32)	59.9
				D(29,27,28,33)	−59.0
				D(30,27,28,31)	59.1
				D(30,27,28,32)	−59.7
				D(30,27,28,33)	−178.6
				D(2,27,29,34)	−63.7

Table 1 (continued)

Bondlengths (Å)	Bondangles (°)	Dihedralangles (°)
		D(2,27,29,35)
		176.7
		D(2,27,29,36)
		56.8
		D(28,27,29,34)
		58.9
		D(28,27,29,35)
		−60.6
		D(28,27,29,36)
		179.4
		D(30,27,29,34)
		178.6
		D(30,27,29,35)
		59.1
		D(30,27,29,36)
		−60.9
		D(2,27,30,37)
		63.8
		D(2,27,30,38)
		−56.7
		D(2,27,30,39)
		−176.7
		D(28,27,30,37)
		−58.9
		D(28,27,30,38)
		−179.4
		D(28,27,30,39)
		60.6
		D(29,27,30,37)
		−178.6
		D(29,27,30,38)
		60.9
		D(29,27,30,39)
		−59.1

The stretching mode of NH group is generally give rise to bands [25,26] in the range 3500–3300  $\text{cm}^{-1}$ . For the title compound the NH stretching mode is observed at 3347  $\text{cm}^{-1}$  in the IR spectrum, and at 3343  $\text{cm}^{-1}$  in the Raman spectrum and theoretical value is 3385  $\text{cm}^{-1}$  (SDD). In mono-substituted amides, the in-plane bending frequency and the resonance stiffened CN band stretching frequency fall close together and therefore interact. The CNH vibration where the nitrogen and the hydrogen move in opposite directions relative to the carbon atom involves both NH bend and CN stretching and absorbs [27] near 1500  $\text{cm}^{-1}$ . This band is very characteristic for mono-substituted amides. The CNH vibration where N and H atoms move in the same direction relative to the carbon atom gives rise to a band [27] near 1250  $\text{cm}^{-1}$ . For the title compound, the bands at 1494, 1249  $\text{cm}^{-1}$  (SDD) are assigned as CNH bending modes. The out-of-plane NH wag is assigned at 825  $\text{cm}^{-1}$  theoretically. Mary et al. [28] reported the NH bands at 1547, 1250, 650  $\text{cm}^{-1}$  in the IR spectrum and at 1580, 1227, 652  $\text{cm}^{-1}$  theoretically for a similar derivative. Aromatic ring with nitrogen directly on the ring absorb at 1330–1260  $\text{cm}^{-1}$  because of the stretching of the phenyl C–N bond [27]. For the title compound, the C<sub>9</sub>–N<sub>18</sub> stretching mode is observed (SDD) at 1237  $\text{cm}^{-1}$ . The C<sub>8</sub>–N<sub>18</sub> stretching band is reported in the range 1000–1200  $\text{cm}^{-1}$  [29] and in the present case this band is observed at 1084  $\text{cm}^{-1}$  theoretically.

The methyl stretching vibrations are expected in the region 3010–2900  $\text{cm}^{-1}$  (asymmetric) and 2950–2850  $\text{cm}^{-1}$  (symmetric) [24]. In the present case the tertiary butyl  $\nu_{\text{as}}\text{CH}_3$  stretching vibrations are observed at 3031, 2980  $\text{cm}^{-1}$  in the IR spectrum and at 3015, 2984  $\text{cm}^{-1}$  in the Raman spectrum. The calculated values for these modes are 3038, 3032, 3014, 3006, 3005, 2999  $\text{cm}^{-1}$  (SDD). The symmetric stretching modes of the methyl group are calculated to be at 2927, 2922, 2917  $\text{cm}^{-1}$  (SDD) and bands are observed at 2934, 2910  $\text{cm}^{-1}$  in IR and 2918  $\text{cm}^{-1}$  in the Raman spectrum. The methyl asymmetric deformations  $\delta_{\text{as}}\text{CH}_3$  absorb [24] between 1495 and 1435  $\text{cm}^{-1}$ . Although three methyl symmetric bending modes are expected often only two emerge experimentally. The asymmetric deformations of the methyl groups are observed at 1486 and 1471  $\text{cm}^{-1}$  experimentally. In the present case the bands observed at 1405, 1362  $\text{cm}^{-1}$  in the IR spectrum and at 1410 in the Raman spectrum are assigned as the symmetric deformations of the methyl group. The SDD calculations give these modes at 1487, 1473, 1466, 1460, 1459, 1446 and 1395, 1369, 1364  $\text{cm}^{-1}$  as asymmetric and symmetric methyl deformations, respectively, for the title compound. Most of the investigated molecules display the first methyl rock [24] in the region 1150 ± 35  $\text{cm}^{-1}$ . The other methyl rocking modes are expected in the region [24] 1035 ± 55, 990 ± 50 and 925 ± 30  $\text{cm}^{-1}$ . The SDD

calculations give these rocking modes of the tBu group at 1188, 1013, 1002 and 966, 920, 906  $\text{cm}^{-1}$ . The tBu group gives rise to five skeletal deformations absorbing in the three regions [24]:  $\delta_{\text{as}}\text{CC}_3$  in 435 ± 85,  $\delta_{\text{s}}\text{CC}_3$  in 335 ± 80 and  $\rho\text{CC}_3$  in 300 ± 80  $\text{cm}^{-1}$ . These modes normally produce bands of weak or medium intensity. The highest (lowest) values for  $\delta_{\text{as}}\text{CC}_3$  are observed [24] around 510 (355)  $\text{cm}^{-1}$ . Most of the  $\delta_{\text{as}}\text{CC}_3$  modes have been assigned in the region [24] 435 ± 65  $\text{cm}^{-1}$ . The SDD calculations give frequencies at 496, 326 and 313  $\text{cm}^{-1}$  as asymmetric and symmetric deformations. The bands at 290, 219  $\text{cm}^{-1}$  (SDD) are assigned as the rocking modes of  $\text{CC}_3$ . The torsion modes  $\tau\text{CH}_3$  and  $\tau\text{CC}_3$  are expected in the low frequency region [24]. The  $\nu_{\text{as}}\text{CC}_3$  and  $\nu_{\text{s}}\text{CC}_3$  modes are expected in the regions 1235 ± 60 and 800 ± 90  $\text{cm}^{-1}$ , respectively [24]. For the title compound the bands observed at 1244  $\text{cm}^{-1}$  in the IR spectrum, 1247  $\text{cm}^{-1}$  in the Raman spectrum and at 1286, 1249  $\text{cm}^{-1}$  theoretically are assigned as  $\nu_{\text{as}}\text{CC}_3$  modes. The SDD calculations give the symmetric  $\nu_{\text{s}}\text{CC}_3$  stretching mode at 906  $\text{cm}^{-1}$  and the bands observed at 907  $\text{cm}^{-1}$  in the IR spectrum, 904  $\text{cm}^{-1}$  in the Raman spectrum are assigned as these modes. These modes are not pure but contain significant contributions from other modes.

The  $\text{CF}_3$  group possesses as many normal vibrations as methyl and as, halogen atoms are much heavier than hydrogen,  $\text{CF}_3$  modes are expected at considerably lower values. According to Roeges [24] the absorption regions of  $-\text{CF}_3$  in substituted benzene are:  $\nu\text{CF}$  1300–1000;  $\delta\text{CF}$  720–440;  $\rho\text{CF}$  470–260 and  $\tau\text{CF}$  below 100  $\text{cm}^{-1}$ . In the present case the bands at 1140, 1026  $\text{cm}^{-1}$  in the IR spectrum, 1142, 1026  $\text{cm}^{-1}$  in the Raman spectrum and at 1132, 1026, 1017  $\text{cm}^{-1}$  (SDD) are assigned as the stretching modes of  $\text{CF}_3$  group. The deformation bands are assigned at 674, 594, 511, 478  $\text{cm}^{-1}$  in the IR spectrum, 672, 601, 520, 475, 395, 372  $\text{cm}^{-1}$  in the Raman spectrum and at 681, 594, 515, 480, 389, 373  $\text{cm}^{-1}$  theoretically. Iriarte et al. [30] reported the  $\text{CF}_3$  stretching values at 1244, 1213, 1140, 1128, (DFT), 1218, 1176, 1136, 1127 (experimental), deformation bands of  $\text{CF}_3$  at 729  $\text{cm}^{-1}$  (experimental), 743  $\text{cm}^{-1}$  (DFT).

The pyrazine CH stretching modes are reported in the range 3100–300  $\text{cm}^{-1}$  [31,32]. The pyrazine CH stretching modes are assigned at 3130, 3123  $\text{cm}^{-1}$  theoretically and experimentally bands are observed at 3117  $\text{cm}^{-1}$  for the title compound. The pyrazine CH stretching modes are reported at 3057, 3070, 3086 (IR), 3060, 3070, 3087 (Raman), 3061, 3074, 3079  $\text{cm}^{-1}$  (theoretical) for 2-chloropyrazine and 3099, 3104 (IR), 3078, 3103 (Raman), 3096, 3100  $\text{cm}^{-1}$  (calculated) for 2,6-dichloropyrazine [1].

For 2-aminopyrazine-3-carboxylic acid [1] the pyrazine ring stretching modes are observed at 1564, 1536, 1468, 1458, 1360, 1258, 1083  $\text{cm}^{-1}$  (Raman) and 1567, 1457, 1415, 1373, 1231,

**Table 2**  
Calculated (scaled) wavenumbers, IR, Raman bands and assignments of 5-*tert*-Butyl-*N*-(4-trifluoromethylphenyl)pyrazine-2-carboxamide.

B3LYP/6-31G*			B3PW91/6-31G*			B3LYP/SDD			IR	Raman	Assignments <sup>a</sup>
$\nu(\text{cm}^{-1})$	IR <sub>i</sub>	R <sub>A</sub>	$\nu(\text{cm}^{-1})$	IR <sub>i</sub>	R <sub>A</sub>	$\nu(\text{cm}^{-1})$	IR <sub>i</sub>	R <sub>A</sub>	$\nu(\text{cm}^{-1})$	$\nu(\text{cm}^{-1})$	
3389	92.21	276.24	3389	121.56	312.49	3385	109.64	305.36	3347	3343	$\nu\text{NH}(99)$
3156	5.61	42.56	3158	5.47	51.44	3149	5.29	47.92	–	3156	$\nu\text{CH}(97)$
3127	9.78	116.69	3140	9.78	110.25	3130	10.29	103.96	–	–	$\nu\text{CH}(99)\text{Pz}$
3123	3.54	39.08	3133	4.56	31.88	3123	3.99	36.03	–	3117	$\nu\text{CH}(99)\text{Pz}$
3114	2.60	115.07	3128	2.24	105.12	3113	2.10	105.79	–	3117	$\nu\text{CH}(98)$
3108	2.54	89.88	3120	2.29	70.13	3105	2.38	68.98	3105	3082	$\nu\text{CH}(97)$
3076	10.35	46.42	3092	9.89	38.58	3076	10.02	38.81	3070	3062	$\nu\text{CH}(99)$
3031	27.52	90.16	3054	36.94	80.19	3038	40.11	81.01	–	–	$\nu_{\text{as}}\text{CH}_3(94)$
3026	1.58	10.41	3050	2.63	10.07	3032	2.60	10.02	3031	–	$\nu_{\text{as}}\text{CH}_3(92)$
3005	78.63	260.82	3032	100.65	227.16	3014	105.31	227.66	–	3015	$\nu_{\text{as}}\text{CH}_3(100)$
2998	8.07	49.22	3026	6.24	34.87	3006	8.70	41.21	–	–	$\nu_{\text{as}}\text{CH}_3(72)$
2997	40.05	46.87	3024	43.36	37.70	3005	51.27	41.92	–	–	$\nu_{\text{as}}\text{CH}_3(99)$
2992	7.92	15.85	3019	11.50	14.72	2999	7.37	10.62	2980	2984	$\nu_{\text{as}}\text{CH}_3$
2932	26.71	330.46	2937	32.22	389.98	2927	29.52	377.30	2934	–	$\nu_3\text{CH}_3(88)$
2927	36.11	3.67	2934	42.36	3.23	2922	40.73	3.15	–	–	$\nu_2\text{CH}_3(100)$
2922	19.31	18.29	2929	24.90	44.10	2917	22.71	28.51	2910	2918	$\nu_2\text{CH}_3(87)$
1635	135.06	465.76	1628	145.87	841.63	1610	152.82	912.27	1613	1617	$\nu\text{CO}(66)$
1613	48.00	268.09	1615	136.18	52.49	1598	92.42	22.22	1599	1599	$\nu\text{Ph}(53)$ , $\nu\text{CO}(16)$
1585	249.66	204.25	1587	138.02	94.16	1572	167.83	84.36	1580	1582	$\nu\text{Ph}(72)$ , $\delta\text{NH}(16)$
1540	88.67	953.87	1543	83.69	990.00	1527	90.89	1004.88	1531	1523	$\delta\text{CH}_3(20)$ , $\nu\text{Pz}(56)$
1527	489.81	477.84	1524	566.20	714.37	1510	533.37	597.96	–	–	$\nu\text{Ph}(61)$ , $\delta\text{NH}(21)$
1514	8.25	23.26	1506	5.82	3.05	1494	12.33	0.97	–	–	$\delta\text{NH}(57)$ , $\nu\text{Ph}(22)$
1506	48.45	7.04	1497	99.27	71.38	1487	97.63	7.39	1486	–	$\delta_{\text{as}}\text{CH}_3(76)$
1495	4.46	72.78	1489	52.45	2.13	1481	18.26	54.20	–	–	$\nu\text{Pz}(63)$
1492	9.38	27.70	1476	15.19	18.14	1473	14.38	17.96	–	1471	$\delta_{\text{as}}\text{CH}_3(88)$
1486	13.17	24.22	1468	14.70	15.10	1466	14.51	14.86	–	–	$\delta_{\text{as}}\text{CH}_3(86)$
1480	0.50	23.84	1461	8.16	19.69	1460	0.90	14.11	–	–	$\delta_{\text{as}}\text{CH}_3(89)$
1478	1.55	24.34	1461	2.48	14.63	1459	4.79	20.09	–	–	$\delta_{\text{as}}\text{CH}_3(87)$
1466	0.02	6.25	1447	61.10	42.10	1446	0.24	4.86	–	–	$\delta_{\text{as}}\text{CH}_3(85)$
1454	54.61	60.12	1447	1.97	5.90	1440	61.45	54.01	–	1445	$\delta\text{CHPz}(46)$ , $\nu\text{Pz}(20)$
1412	4.56	3.35	1405	91.14	48.32	1395	106.37	54.22	1405	1410	$\delta_2\text{CH}_3(91)$
1410	109.27	70.22	1395	8.46	10.23	1395	6.44	12.42	–	–	$\nu\text{Ph}(41)$ , $\delta\text{CH}(36)$
1386	12.03	7.10	1368	27.05	1.62	1369	21.94	3.23	–	–	$\delta_2\text{CH}_3(94)$
1381	9.07	2.27	1364	18.45	0.45	1364	17.18	0.41	1362	–	$\delta_2\text{CH}_3(96)$
1336	105.72	402.50	1353	115.82	292.89	1334	120.14	337.38	1328	1336	$\nu\text{Ph}(65)$
1325	0.11	16.44	1312	8.41	103.98	1309	10.25	73.06	–	1312	$\nu\text{Ph}(18)$ , $\delta\text{CH}(63)$
1309	28.18	9.88	1303	45.05	4.87	1291	22.54	3.61	1293	1291	$\nu\text{Pz}(66)$
1295	527.63	132.71	1289	0.12	13.65	1286	0.39	4.95	–	–	$\nu_{\text{as}}\text{CC}_3(57)$ , $\nu\text{Pz}(17)$
1293	33.82	7.30	1282	519.11	118.87	1270	28.08	125.14	–	–	$\delta\text{CHPz}(62)$
1275	42.48	14.21	1281	45.24	140.80	1269	575.98	128.51	1268	1270	$\nu\text{C}_{27}(47)$ , $\delta\text{CH}_3(28)$
1261	18.85	364.74	1257	16.14	147.85	1249	0.68	280.22	1244	1247	$\delta\text{NH}(48)$ , $\nu_{\text{as}}\text{CC}_3(37)$
1250	65.65	342.25	1246	62.96	417.35	1237	63.15	399.36	–	–	$\nu\text{C}_9\text{N}_{18}(50)$ , $\delta\text{CHPz}(24)$
1211	6.21	32.40	1224	15.27	68.74	1207	9.52	48.01	1213	–	$\nu\text{Pz}(53)$ , $\delta\text{CH}_3(18)$
1195	2.41	10.36	1199	2.46	16.22	1188	3.09	16.76	1190	1192	$\delta\text{CH}_3(84)$
1193	56.68	124.40	1193	30.37	1.98	1183	64.79	144.33	–	–	$\delta\text{CH}(73)$
1186	15.11	0.25	1186	36.50	116.04	1177	17.63	0.61	1162	–	$\nu\text{Pz}(67)$
1152	36.70	7.82	1137	59.43	32.23	1132	54.83	33.47	1140	1142	$\nu\text{CF}_3(53)$ , $\delta\text{CH}(32)$
1146	77.89	33.30	1130	38.09	12.11	1126	52.57	19.37	1120	1124	$\nu\text{Pz}(79)$
1105	36.86	24.74	1093	4.64	29.97	1084	3.62	29.97	1070	1069	$\nu\text{CF}_3(16)$ , $\nu\text{Pz}(14)$ , $\nu\text{C}_8\text{N}_{18}(47)$
1092	111.78	10.12	1039	194.89	1.93	1026	188.36	1.85	1026	1026	$\nu\text{CF}_3(69)$
1084	236.56	21.15	1023	103.59	2.92	1017	1.33	5.74	–	–	$\nu\text{CF}_3(71)$
1035	125.00	5.54	1019	1.56	5.83	1015	91.52	3.79	–	–	$\delta\text{CH}(46)$ , $\nu\text{CF}_3(22)$ , $\delta\text{CF}_3(16)$
1031	0.74	3.66	1016	2.81	10.89	1013	4.07	11.19	–	–	$\delta\text{CH}_3(72)$
1028	4.28	9.23	1003	140.86	20.32	1002	27.10	2.72	–	–	$\delta\text{CH}_3(67)$
1006	69.79	6.97	997	54.95	11.62	989	134.95	25.56	–	987	$\delta\text{Ph}(56)$ , $\nu\text{Ph}(18)$
999	44.42	2.76	987	15.81	4.52	982	15.80	3.98	–	–	$\delta\text{Pz}(41)$ , $\nu\text{Pz}(29)$
993	1.16	1.37	982	179.29	2.99	976	201.00	5.71	979	–	$\gamma\text{CH}(85)$
960	1.60	2.01	969	1.72	0.39	967	2.12	0.47	–	–	$\gamma\text{CHPz}(81)$
957	0.22	0.11	967	7.25	1.84	966	28.86	4.77	958	962	$\delta\text{CH}_3(95)$
956	0.39	1.89	944	0.24	0.01	943	0.14	0.01	–	–	$\gamma\text{CH}(82)$ , $\tau\text{Ph}(11)$
924	4.67	0.33	934	8.31	0.28	930	9.77	0.31	927	934	$\gamma\text{CHPz}(68)$
924	1.42	11.07	928	3.14	8.36	920	2.46	9.82	–	–	$\nu\text{C}12\text{C}22(49)$ , $\delta\text{CH}_3(32)$
905	0.33	11.94	916	1.25	9.50	906	1.04	11.12	907	904	$\delta\text{CH}_3(32)$ , $\nu_2\text{CC}_3(52)$

Table 2 (continued)

B3LYP/6-31G*			B3PW91/6-31G*			B3LYP/SDD			IR	Raman	Assignments <sup>a</sup>
$\nu(\text{cm}^{-1})$	IR <sub>I</sub>	R <sub>A</sub>	$\nu(\text{cm}^{-1})$	IR <sub>I</sub>	R <sub>A</sub>	$\nu(\text{cm}^{-1})$	IR <sub>I</sub>	R <sub>A</sub>	$\nu(\text{cm}^{-1})$	$\nu(\text{cm}^{-1})$	
879	21.41	13.31	871	128.70	1.29	870	115.37	1.56	–	–	$\delta\text{NH}(37)$ , $\delta\text{CO}(48)$
866	111.17	1.89	867	19.15	16.87	861	18.32	17.64	–	859	$\gamma\text{CH}(66)$
845	63.56	4.76	851	79.41	0.39	847	86.32	0.49	843	842	$\gamma\text{CH}(71)$ , $\gamma\text{NH}(14)$
838	4.83	12.88	833	5.62	8.75	825	5.61	9.88	–	–	$\gamma\text{NH}(51)$ , $\nu\text{CC}(13)$
819	1.90	15.14	818	3.11	9.35	814	3.75	1.98	–	–	$\nu\text{CC}(42)$ , $\nu\text{C}_2\text{C}_{27}(22)$
812	1.43	3.33	818	3.21	10.91	810	3.56	16.90	809	812	$\tau\text{Pz}(52)$ , $\gamma\text{CC}(27)$
789	27.33	0.25	800	11.89	0.81	792	20.53	0.63	781	780	$\gamma\text{NH}(37)$ , $\nu\text{Ph}(48)$
759	17.78	48.32	750	22.37	59.13	745	22.99	62.84	749	–	$\delta\text{Pz}(29)$ , $\nu\text{CC}(29)$
735	1.73	1.80	744	2.65	1.09	739	2.97	1.03	729	737	$\tau\text{Ph}(65)$ , $\delta\text{CN}(13)$ , $\gamma\text{CC}(11)$
704	0.01	2.57	712	0.66	0.76	708	0.65	0.84	–	698	$\gamma\text{CO}(43)$ , $\tau\text{Pz}(11)$ , $\gamma\text{CC}(17)$
699	8.75	4.68	686	4.58	8.32	681	3.80	8.92	674	672	$\nu\text{CF}_3(42)$ , $\delta\text{Ph}(28)$
641	0.32	4.67	626	1.05	5.32	626	0.75	5.07	630	635	$\delta\text{Ph}(77)$
638	4.63	21.69	624	4.21	24.03	624	5.00	25.37	–	–	$\delta\text{Pz}(78)$
608	5.15	2.53	597	4.98	2.92	594	4.56	3.49	594	601	$\delta\text{CF}_3(32)$ , $\delta\text{Ph}(31)$
578	14.79	0.97	573	25.56	0.88	571	21.92	0.94	–	578	$\gamma\text{CN}(22)$ , $\tau\text{Ph}(19)$ , $\gamma\text{CC}(12)$
567	3.65	0.65	564	4.18	0.72	563	4.91	0.73	566	–	$\tau\text{Pz}(37)$ , $\gamma\text{CC}(34)$
566	0.80	1.08	560	0.30	0.61	557	0.17	0.80	538	–	$\tau\text{CO}(46)$ , $\delta\text{CC}(25)$
531	0.13	1.90	519	0.05	1.93	515	0.05	2.22	511	520	$\delta\text{CF}_3(45)$ , $\delta\text{CC}(22)$
504	1.03	9.32	498	0.95	8.22	496	0.91	7.82	490	501	$\delta\text{asCC}(366)$
486	1.02	1.14	483	2.81	0.96	480	2.42	0.99	478	475	$\delta\text{CF}_3(41)$ , $\tau\text{Ph}(35)$
449	2.34	1.41	442	1.44	1.37	441	1.62	1.48	444	–	$\delta\text{CH}_3(43)$ , $\delta\text{CC}(22)$
425	18.20	0.13	422	17.46	0.16	424	16.73	0.17	418	428	$\tau\text{Pz}(72)$
415	0.16	0.09	409	0.13	0.05	409	0.08	0.04	408	–	$\tau\text{Ph}(81)$
397	2.71	1.39	391	3.18	1.56	389	2.98	1.55	–	395	$\delta\text{CF}_3(56)$ , $\tau\text{Pz}(32)$
392	19.43	4.35	385	20.79	5.18	383	20.47	5.44	–	–	$\delta\text{CF}_3(44)$ , $\delta\text{CN}(30)$
382	1.65	2.59	373	1.70	2.67	373	0.98	2.59	–	372	$\delta\text{CF}_3(46)$ , $\delta\text{CH}_3(22)$
376	0.51	1.35	370	0.78	1.39	370	0.86	1.60	–	–	$\delta\text{CH}_3(29)$ , $\tau\text{Pz}(24)$ , $\delta\text{CF}_3(15)$
350	16.00	0.48	341	14.71	0.44	341	16.07	0.49	–	–	$\delta\text{CO}(23)$ , $\delta\text{NH}(22)$ , $\delta\text{CF}_3(21)$
331	1.84	1.40	326	1.62	1.10	326	1.62	1.10	–	333	$\delta\text{CH}_3(36)$ , $\delta\text{asCC}_3(37)$
322	1.04	3.94313	313	4.12	313	1.16	4.32	–	306	–	$\delta\text{CH}_3(33)$ , $\delta\text{sCC}_3(44)$
301	0.02	0.01	298	0.01	0.01	290	0.01	0.01	–	286	$\tau\text{CC}_3(81)$
285	0.45	0.56	280	0.10	0.44	278	0.02	0.43	–	–	$\tau\text{CC}_3(43)$ , $\delta\text{CC}(10)$
279	5.70	0.13	271	4.73	0.11	270	6.42	0.26	–	–	$\tau\text{CC}(41)$ , $\delta\text{CC}(29)$
263	5.60	0.92	256	7.15	1.26	256	5.14	1.14	–	258	$\delta\text{CC}(38)$ , $\tau\text{CC}(37)$
252	0.50	0.41	249	0.69	0.36	248	0.66	0.41	–	–	$\tau\text{Ph}(33)$ , $\delta\text{CF}_3(16)$ , $\tau\text{CC}(23)$
236	0.15	0.33	225	0.10	0.78	219	0.10	0.93	–	222	$\tau\text{CC}(71)$
196	1.38	1.55	191	1.28	3.58	191	1.32	3.27	–	195	$\delta\text{CC}(36)$ , $\delta\text{NH}(11)$ , $\delta\text{CF}_3(16)$
195	0.95	3.76	189	1.04	1.05	190	1.03	1.32	–	–	$\delta\text{CC}(32)$ , $\gamma\text{CC}(44)$
160	0.80	0.54	157	0.73	0.80	157	0.79	0.86	–	165	$\delta\text{CC}(39)$ , $\delta\text{Ph}(32)$
130	0.91	1.49	130	0.93	1.39	129	0.93	1.39	–	–	$\delta\text{CC}(22)$ , $\tau\text{CC}(21)$ , $\gamma\text{NH}(17)$
125	2.95	0.75	121	3.37	0.76	122	3.25	0.79	–	115	$\delta\text{CC}(17)$ , $\tau\text{CO}(47)$
86	2.62	0.43	84	2.78	0.31	84	2.97	0.31	–	87	$\tau\text{CN}(57)$ , $\gamma\text{CC}(11)$
67	0.35	0.20	68	0.49	0.36	68	0.39	0.38	–	–	$\tau\text{CC}(30)$ , $\tau\text{CN}(29)$ , $\tau\text{Pz}(20)$
54	0.59	0.95	53	0.87	0.42	53	0.83	0.45	–	–	$\tau\text{CN}(38)$ , $\tau\text{Pz}(25)$
46	0.06	0.31	44	0.06	0.29	44	0.05	0.30	–	–	$\delta\text{CCN}(27)$ , $\delta\text{NH}(21)$ , $\delta\text{CC}(21)$
35	1.27	6.27	32	1.07	4.59	32	1.10	4.57	–	–	$\tau\text{CC}(61)$
20	0.01	0.03	20	0.02	0.02	21	0.02	0.02	–	–	$\tau\text{CN}(29)$ , $\gamma\text{NH}(11)$ , $\tau\text{CC}(21)$
14	0.13	0.32	13	0.21	0.77	10	0.23	0.85	–	–	$\tau\text{CC}(59)$ , $\delta\text{CC}(11)$

<sup>a</sup> % Of PED is given in the brackets with the assignments. Abbreviations- $\nu$ -stretching;  $\delta$ -in-plane deformation;  $\gamma$ -out-of-plane deformation;  $\tau$ -twisting; s-symmetric; as-asymmetric; Ph-benzenering; Pz-pyrazinering; IR<sub>I</sub> – IR intensity; R<sub>A</sub> – Raman activity.

1068  $\text{cm}^{-1}$  (theoretical). For pyrazine, the ring stretching modes are reported at 1485, 1411, 1128, 1065 (IR), 1579, 1522, 1015 (Raman) and 1597, 1545, 1482, 1412, 1140, 1063, 1009  $\text{cm}^{-1}$  theoretically [1]. For the title compound the pyrazine ring stretching modes are observed at 1531, 1293, 1213, 1162  $\text{cm}^{-1}$  in the IR spectrum, 1523, 1291  $\text{cm}^{-1}$  in the Raman spectrum and at 1527, 1481, 1291, 1207, 1177  $\text{cm}^{-1}$  theoretically (SDD). The ring breathing mode of the pyrazine ring is observed at 1120  $\text{cm}^{-1}$  in the IR spectrum, 1124  $\text{cm}^{-1}$  in the Raman spectrum and at 1126  $\text{cm}^{-1}$  theoretically. The ring breathing mode of pyrazine is reported at 1015  $\text{cm}^{-1}$  [1]. In the Raman spectrum of 2,6-dichloropyrazine and 2-chloropyrazine the ring breathing mode is reported at 1131 and 1049  $\text{cm}^{-1}$  [1]. For the title compound the in-plane and out-of-plane CH bending modes are assigned at 1440, 1270 and

967, 930  $\text{cm}^{-1}$  (SDD) theoretically. Corresponding bands observed at 927 in the IR spectrum and at 1445, 934  $\text{cm}^{-1}$  in the Raman spectrum which is in agreement with literature [1].

The benzene ring possesses six ring stretching modes, of which the four with the highest wavenumbers (occurring near 1600, 1580, 1490 and 1440  $\text{cm}^{-1}$ ) are good group vibrations [24]. With heavy substituents, the bands tend to shift to somewhat lower wavenumbers. In the absence of ring conjugation, the band at 1580  $\text{cm}^{-1}$  is usually weaker than at 1600  $\text{cm}^{-1}$ . In the case of C=O substitution, the band near 1490  $\text{cm}^{-1}$  can be very weak. The fifth ring stretching mode is active near 1315  $\pm$  65  $\text{cm}^{-1}$ , a region that overlaps strongly with that of the CH in-plane deformation. The sixth ring stretching mode or the ring breathing mode, appears as a weak band near 1000  $\text{cm}^{-1}$  in mono-, 1,3-di and

1,3,5-trisubstituted benzenes [24]. In the otherwise substituted benzenes, however, this mode is substituent sensitive and difficult to distinguish from the ring in-plane deformation [24]. The  $\nu_{\text{Ph}}$  modes are expected in the range 1280–1630  $\text{cm}^{-1}$  for para substituted phenyl rings [24] and the modes observed at 1599, 1580, 1328  $\text{cm}^{-1}$  in the IR spectrum, 1599, 1582, 1336  $\text{cm}^{-1}$  in the Raman spectrum and at 1598, 1572, 1510, 1395, 1334  $\text{cm}^{-1}$  theoretically (SDD) are assigned as  $\nu_{\text{Ph}}$  modes. The ring breathing mode of the para substituted benzenes with entirely different substituents [33] has been reported in the interval 780–880  $\text{cm}^{-1}$ . For the title compound, this is confirmed by the band in the infrared spectrum at 781  $\text{cm}^{-1}$  and at 792  $\text{cm}^{-1}$  theoretically, which finds support from computational results. For para substituted benzene, the ring breathing mode was reported at 804 and 792  $\text{cm}^{-1}$  experimentally and at 782 and 795  $\text{cm}^{-1}$  theoretically [34,35].

The CH in-plane deformation bands of the benzene ring are expected above 1000  $\text{cm}^{-1}$  [24] and in the present case, the bands observed at 1140  $\text{cm}^{-1}$  in the IR spectrum, 1312, 1142  $\text{cm}^{-1}$  in the Raman spectrum and at 1309, 1183, 1132, 1015  $\text{cm}^{-1}$  theoretically are assigned as these modes. The out-of-plane CH deformations of the phenyl ring [24] are observed between 1000 and 700  $\text{cm}^{-1}$ . Generally, the CH out-of-plane deformations with the highest wavenumbers have weaker intensity than those absorbing at lower wavenumbers. The CH out-of-plane vibrations are observed at 979, 843  $\text{cm}^{-1}$  in the IR spectrum, 859, 842  $\text{cm}^{-1}$  in the Raman spectrum and at 976, 943, 861, 847  $\text{cm}^{-1}$  theoretically. The strong  $\gamma_{\text{CH}}$  occurring at  $840 \pm 50 \text{ cm}^{-1}$ , is typical for 1,4-disubstitution, and the band observed at 843  $\text{cm}^{-1}$  in the IR spectrum is assigned to this mode. The SDD calculations give this mode at 847  $\text{cm}^{-1}$ . The substituent sensitive modes and other deformation bands of the phenyl and pyrazine ring are also identified and assigned (Table 2). Most of the modes are not pure, but contain significant contributions from other modes.

#### Geometrical parameters and first hyperpolarizability

To the best of our knowledge, no X-ray crystallographic data of the title compound has yet been established. However, the theoretical results obtained are almost comparable with the reported structural parameters of similar molecules. In the case of 2-amino-pyrazine-3-carboxylic acid the bond lengths  $\text{C}_5\text{--C}_8$ ,  $\text{C}_8\text{--O}_{19}$ ,  $\text{C}_5\text{--N}_6$ ,  $\text{C}_5\text{--C}_4$  are 1.479, 1.212, 1.333, 1.4079 Å (XRD) and 1.492, 1.186, 1.315, 1.4092 Å (ab initio calculations) [12,36]. In the present case, the corresponding values are 1.505, 1.2586, 1.3581 and 1.4097. For pyrazine ring [37] the CN bond lengths are 1.339 and 1.331 Å. For 2-chloropyrazine [1] CN bond lengths are in the range 1.335–1.312 Å. For the title compound, the pyrazine bond lengths  $\text{C}_1\text{--C}_2$ ,  $\text{C}_1\text{--N}_6$ ,  $\text{C}_5\text{--N}_6$ ,  $\text{C}_5\text{--C}_4$ ,  $\text{C}_4\text{--N}_3$  and  $\text{C}_2\text{--N}_3$  are 1.4185, 1.3522, 1.3581, 1.4097, 1.3509, 1.367 Å, respectively. For a similar derivative Mary et al. [28] reported the corresponding values as 1.3917, 1.2996, 1.3229, 1.3840, 1.322 and 1.3116 Å. Endredi et al. [38] reported the bond lengths  $\text{C}_2\text{--C}_1$ ,  $\text{C}_1\text{--N}_6$ ,  $\text{C}_5\text{--N}_6$ ,  $\text{C}_5\text{--C}_4$  and  $\text{C}_4\text{--N}_3$  as 1.391, 1.331, 1.331, 1.331 and 1.331 Å for pyrazine, 1.4, 1.327, 1.333, 1.387 and 1.334 Å for 2-methylpyrazine, 1.41, 1.331, 1.33, 1.385 and 1.331 Å for 2,3-dimethylpyrazine, 1.396, 1.327, 1.335, 1.396 and 1.335 Å for 2,5-dimethylpyrazine, and 1.399, 1.326, 1.332, 1.399 and 1.332 Å for 2,6-dimethylpyrazine. For pyrazinamide, Chis et al. [39] reported bond lengths,  $\text{C}_5\text{--N}_6$ ,  $\text{C}_4\text{--C}_5$ ,  $\text{C}_4\text{--N}_3$ ,  $\text{C}_2\text{--N}_3$ ,  $\text{C}_1\text{--C}_2$ ,  $\text{C}_1\text{--N}_6$ ,  $\text{C}_5\text{--C}_8$ ,  $\text{C}_8\text{--N}_{18}$ ,  $\text{C}_8\text{--O}_{19}$ ,  $\text{C}_4\text{--H}_7$ ,  $\text{N}_{18}\text{--H}_{20}$  as 1.341, 1.4, 1.337, 1.338, 1.397, 1.336, 1.510, 1.357, 1.226, 1.086, 1.010 Å and these results are in agreement with the present study.

The CN bond length in the pyrazine ring of the title compound  $\text{C}_1\text{--N}_6 = 1.3522$ ,  $\text{C}_5\text{--N}_6 = 1.3581$ ,  $\text{C}_2\text{--N}_3 = 1.3670$  and  $\text{C}_4\text{--N}_3 = 1.3509$  Å are much shorter than the normal C–N single bond that is referred to 1.49 Å. The same results are shown for

the bond lengths of the two C–C bonds,  $\text{C}_2\text{--C}_1 = 1.4185$  and  $\text{C}_5\text{--C}_4 = 1.4097$  Å in the pyrazine ring and are also smaller than that of the normal C–C single bond of 1.54 Å [40]. The C–N bond lengths  $\text{C}_8\text{--N}_{18} = 1.3797$  and  $\text{C}_9\text{--N}_{18} = 1.4109$  Å are also shorter than the normal C–N single bond of 1.49 Å, which confirms this bond to have some character of a double or conjugated bond [41].

At  $\text{N}_{18}$  position, the angles  $\text{C}_8\text{--N}_{18}\text{--H}_{20}$  is 113.3°,  $\text{C}_9\text{--N}_{18}\text{--H}_{20}$  is 118.1° and  $\text{C}_8\text{--N}_{18}\text{--C}_9$  is 128.6°. This asymmetry of angles at  $\text{N}_{18}$  position indicates the weakening of  $\text{N}_{18}\text{--H}_{20}$  bond resulting in proton transfer to the oxygen atom  $\text{O}_{19}$  [42]. The CCF angles lie in the range 112.8–113.2° and the FCF angles in the range 105.2–106.7°, which are in agreement with reported literature [30]. The CF bond lengths are reported as 1.4068, 1.3284, 1.3251, 1.3284 Å theoretically [43,44] and for the title compound the CF lengths are in the range 1.4042–1.4168 Å.

Due to C(CH<sub>3</sub>) substitution in the pyrazine ring the  $\text{C}_1\text{--C}_2$  bond length (1.4185 Å) is greater than the  $\text{C}_4\text{--C}_5$  (1.4097 Å) bond length. The methyl substituent affects all the CN and CC bond lengths of the pyrazine ring of the title compound in comparison with the corresponding bonds of pyrazine [38]. At the  $\text{C}_2$  position of the pyrazine ring, there is asymmetry between the angles,  $\text{C}_1\text{--C}_2\text{--C}_{27}$  (124.3°) and  $\text{N}_3\text{--C}_2\text{--C}_{27}$  (116.5°) due to steric hindrance between  $\text{H}_{26}$  and the tBu group.

For benzamide derivatives, Noveron et al. [45] reported the bond lengths  $\text{C}_9\text{--N}_{18}$ ,  $\text{C}_8\text{--O}_{19}$ ,  $\text{C}_8\text{--N}_{18}$ ,  $\text{C}_8\text{--C}_5$  and  $\text{N}_{18}\text{--H}_{20}$  as 1.3953, 1.2253, 1.3703, 1.4943, 0.733 Å, whereas the corresponding values for the title compound are 1.4109, 1.2586, 1.3797, 1.505, 1.021 Å. The C=O and CN bond lengths [46] in benzamide, acetamide and formamide are respectively, 1.2253, 1.2203, 1.2123 Å and 1.3801, 1.3804, 1.3683 Å. According to literature [47,48] the changes in bond lengths in C=O and CN are consistent with the following interpretation: that is, hydrogen bond decreases the double bond character of C=O bond and increases the double bond character of C–N bond. At  $\text{C}_9$  position the angles  $\text{C}_{10}\text{--C}_9\text{--N}_{18}$  is increased by 3.0° and  $\text{C}_{14}\text{--C}_9\text{--N}_{18}$  is reduced by 2.6° from 120° and this asymmetry reveals the interaction between the amide moiety and the phenyl ring. The CC bond lengths in the phenyl ring lie between 1.3982 and 1.4168 Å and the CH bond lengths between 1.0819 and 1.0877 Å. The CC bond length of benzene [49] is 1.3993 and benzaldehyde [50] 1.3973 Å.

The first hyperpolarizability ( $\beta_0$ ) of this novel molecular system is calculated using B3LYP/6-31G\* method, based on the finite field approach. In the presence of an applied electric field, the energy of a system is a function of the electric field. First hyperpolarizability is a third rank tensor that can be described by a  $3 \times 3 \times 3$  matrix. The 27 components of the 3D matrix can be reduced to 10 components due to the Kleinman symmetry [51]. The components of  $\beta$  are defined as the coefficients in the Taylor series expansion of the energy in the external electric field. When the electric field is weak and homogeneous, this expansion becomes

$$E = E_0 - \sum_i \mu_i F^i - \frac{1}{2} \sum_{ij} \alpha_{ij} F^i F^j - \frac{1}{6} \sum_{ijk} \beta_{ijk} F^i F^j F^k - \frac{1}{24} \sum_{ijkl} \gamma_{ijkl} F^i F^j F^k F^l + \dots$$

where  $E_0$  is the energy of the unperturbed molecule,  $F^i$  is the field at the origin,  $\mu_i$ ,  $\alpha_{ij}$ ,  $\beta_{ijk}$  and  $\gamma_{ijkl}$  are the components of dipole moment, polarizability, the first hyper polarizabilities, and second hyperpolarizabilities, respectively. The calculated first hyperpolarizability of the title compound is  $3.97 \times 10^{-30}$  esu. The C–N distances in the calculated molecular structure vary from 1.3509 to 1.4109 Å which are intermediate between those of a C–N single bond (1.48 Å) and a C=N double bond (1.28 Å). Therefore, the calculated data suggest an extended  $\pi$ -electron delocalization over the pyrazine ring and carboxamide moiety [52] which is responsible for the nonlinearity of the molecule. We conclude that the title compound is an attractive object for future studies of non linear optical properties.

In order to investigate the performance of vibrational wavenumbers of the title compound, the root mean square (RMS) value between the calculated and observed wavenumbers were calculated. The RMS values of wavenumbers were calculated using the following expression [53].

$$\text{RMS} = \sqrt{\frac{1}{n-1} \sum_i^n (v_i^{\text{calc}} - v_i^{\text{exp}})^2}$$

The RMS error of the observed IR and Raman bands are found to 18.42, 16.36 for B3LYP/6-31G\*, 15.38, 14.23 for B3PW91/6-31G\* and 9.25, 9.27 for B3LYP/SDD methods, respectively. The small differences between experimental and calculated vibrational modes are observed. This is due to the fact that experimental results belong to solid phase and theoretical calculations belong to gaseous phase.

### NBO analysis

The natural bond orbitals (NBO) calculations were performed using NBO 3.1 program [54] as implemented in the Gaussian 09 package at the DFT/B3LYP level in order to understand various second-order interactions between the filled orbitals of one subsystem and vacant orbitals of another subsystem, which is a measure of the intermolecular delocalization or hyper-conjugation. NBO analysis provides the most accurate possible natural Lewis structure picture of 'j' because all orbital details are mathematically chosen to include the highest possible percentage of the electron density. A useful aspect of the NBO method is that it gives information about interactions of both filled and virtual orbital spaces that could enhance the analysis of intra and inter molecular interactions.

The second-order Fock-matrix was carried out to evaluate the donor-acceptor interactions in the NBO basis. The interactions re-

sult in a loss of occupancy from the localized NBO of the idealized Lewis structure into an empty non-Lewis orbital. For each donor (i) and acceptor (j) the stabilization energy  $E(2)$  associated with the delocalization  $i \rightarrow j$  is determined as

$$E(2) = \Delta E_{ij} = q_i \frac{(F_{ij})^2}{(E_j - E_i)}$$

$q_i$ , donor orbital occupancy;  $E_i$ ,  $E_j$ , diagonal elements;  $F_{ij}$ , the off diagonal NBO Fock matrix element.

In NBO analysis large  $E(2)$  value shows the intensive interaction between electron-donors and electron-acceptors and greater the extent of conjugation of the whole system, the possible intensive interactions are given in Table 3. The second-order perturbation theory analysis of Fock matrix in NBO basis shows strong intra-molecular hyper-conjugative interactions of  $\pi$  electrons. The intra-molecular hyper-conjugative interactions are formed by the orbital overlap between  $n(\text{C})$  and  $\sigma^*(\text{C}-\text{N})$  bond orbital which results in ICT causing stabilization of the system. The strong intra-molecular hyper-conjugative interaction of  $\text{C}_1-\text{N}_6$ ,  $\text{N}_3-\text{C}_4$  from of  $n1(\text{C}_2) \rightarrow \pi^*(\text{C}_1-\text{N}_6)$  which increases ED (0.36808e) that weakens the respective bonds leading to stabilization of 100.89 kcal mol<sup>-1</sup>. Also the strong intra-molecular hyper-conjugative interaction of  $\text{C}_1-\text{N}_6$ ,  $\text{N}_3-\text{C}_4$  from of  $n1(\text{C}_5) \rightarrow \pi^*(\text{N}_3-\text{C}_4)$  which increases ED (0.32213e) that weakens the respective bonds leading to stabilization of 84.99 kcal mol<sup>-1</sup>. Another intra-molecular hyper-conjugative interactions are formed by the orbital overlap between  $n(\text{N})$  and  $\pi^*(\text{C}-\text{O})$  bond orbital which results in ICT causing stabilization of the system. The strong intra-molecular hyper-conjugative interaction of  $\text{C}_8-\text{O}_{19}$  from of  $n1(\text{N}_{18}) \rightarrow \pi^*(\text{C}_8-\text{O}_{19})$  which increases ED (0.32658e) that weakens the respective bonds leading to stabilization of 67.86 kcal mol<sup>-1</sup>. These interactions are observed as an increase in electron density (ED) in C–O anti-bonding orbitals that weakens the respective bonds. The increased electron density at the nitrogen, carbon atoms leads to the elongation of

**Table 3**

Second-order perturbation theory analysis of Fock matrix in NBO basis corresponding to the intramolecular bonds of the title compound.

Donor (i)	Type	ED/e	Acceptor (j)	Type	ED/e	$E(2)^a$	$E(j)-E(i)^b$	$F(i,j)^c$
$\text{C}_1-\text{N}_6$	$\sigma$	1.98361	$\text{C}_5-\text{C}_8$	$\sigma^*$	0.06866	3.65	1.23	0.061
$\text{C}_1-\text{N}_6$	$\sigma$	1.71948	$\text{C}_5$	$n$	0.98894	47.93	0.18	0.103
$\text{N}_3-\text{C}_4$	$\sigma$	1.98230	$\text{C}_2-\text{C}_{27}$	$\sigma^*$	0.04709	4.07	1.22	0.063
$\text{N}_3-\text{C}_4$	$\pi$	1.69101	$\text{C}_2$	$n$	0.89702	51.59	0.19	0.104
$\text{C}_5-\text{C}_8$	$\sigma$	1.96777	$\text{C}_9-\text{N}_{18}$	$\sigma^*$	0.03234	6.19	1.06	0.072
$\text{C}_8-\text{O}_{19}$	$\pi$	1.97049	$\text{C}_5$	$n$	0.98894	8.09	0.22	0.055
$\text{C}_9-\text{C}_{10}$	$\pi$	1.60844	$\text{C}_{11}-\text{C}_{12}$	$\pi^*$	0.38796	25.75	0.28	0.076
$\text{C}_{10}-\text{C}_{11}$	$\pi$	1.97477	$\text{C}_4-\text{C}_5$	$\pi^*$	0.03234	5.04	1.08	0.066
$\text{C}_{11}-\text{C}_{12}$	$\pi$	1.66648	$\text{C}_{13}-\text{C}_{14}$	$\pi^*$	0.30629	23.61	0.29	0.074
$\text{N}_{18}-\text{H}_{20}$	$\sigma$	1.98027	$\text{C}_8-\text{O}_{19}$	$\sigma^*$	0.01075	5.17	1.14	0.069
$\text{C}_{22}-\text{F}_{23}$	$\sigma$	1.98887	$\text{C}_{12}-\text{C}_{13}$	$\sigma^*$	0.02398	2.39	1.46	0.053
$\text{C}_{22}-\text{F}_{24}$	$\sigma$	1.98890	$\text{C}_{11}-\text{C}_{12}$	$\sigma^*$	0.02410	2.47	1.47	0.054
$\text{LP}(1)\text{C}_2$	$\sigma$	0.89702	$\text{C}_1-\text{N}_6$	$\pi^*$	0.36808	100.89	0.10	0.113
$\text{LP}(1)\text{N}_3$	$n$	1.92760	$\text{C}_4-\text{C}_5$	$\sigma^*$	0.04088	10.74	0.84	0.085
$\text{LP}(1)\text{C}_5$	$\sigma$	0.98894	$\text{N}_3-\text{C}_4$	$\pi^*$	0.32213	84.99	0.13	0.114
$\text{LP}(1)\text{N}_6$	$n$	1.91986	$\text{C}_4-\text{C}_5$	$\sigma^*$	0.04088	10.05	0.86	0.084
$\text{LP}(1)\text{N}_{18}$	$n$	1.63050	$\text{C}_8-\text{O}_{19}$	$\pi^*$	0.32658	67.86	0.25	0.117
$\text{LP}(1)\text{O}_{19}$	$n$	1.97563	$\text{C}_5-\text{C}_8$	$\sigma^*$	0.06866	2.70	1.07	0.049
$\text{LP}(2)\text{O}_{19}$	$n$	1.88860	$\text{C}_8-\text{N}_{18}$	$\sigma^*$	0.06856	22.15	0.67	0.110
$\text{LP}(1)\text{F}_{23}$	$n$	1.98877	$\text{C}_{12}-\text{C}_{22}$	$\sigma^*$	0.05079	0.85	1.44	0.032
$\text{LP}(2)\text{F}_{23}$	$n$	1.96205	$\text{C}_{22}-\text{F}_{25}$	$\sigma^*$	0.12193	5.06	0.53	0.047
$\text{LP}(3)\text{F}_{23}$	$n$	1.94289	$\text{C}_{22}-\text{F}_{24}$	$\sigma^*$	0.10051	10.49	0.53	0.067
$\text{LP}(1)\text{F}_{24}$	$n$	1.98882	$\text{C}_{12}-\text{C}_{22}$	$\sigma^*$	0.05079	0.85	1.44	0.032
$\text{LP}(2)\text{F}_{24}$	$n$	1.96241	$\text{C}_{22}-\text{F}_{25}$	$\sigma^*$	0.12193	4.92	0.53	0.047
$\text{LP}(3)\text{F}_{24}$	$n$	1.94369	$\text{C}_{22}-\text{F}_{23}$	$\sigma^*$	0.10037	10.28	0.53	0.067
$\text{LP}(1)\text{F}_{25}$	$n$	1.98904	$\text{C}_{12}-\text{C}_{22}$	$\sigma^*$	0.05079	0.75	1.44	0.030
$\text{LP}(2)\text{F}_{25}$	$n$	1.96241	$\text{C}_{12}-\text{C}_{22}$	$\sigma^*$	0.05079	4.59	0.77	0.053
$\text{LP}(3)\text{F}_{25}$	$n$	1.94334	$\text{C}_{12}-\text{F}_{24}$	$\sigma^*$	0.10051	9.23	0.52	0.063

<sup>a</sup>  $E(2)$  means energy of hyper-conjugative interactions (stabilization energy in kcalmol<sup>-1</sup>).

<sup>b</sup> Energy difference between donor and acceptor  $i$  and  $j$  NBO orbitals in a.u.

<sup>c</sup>  $F(i,j)$  is the Fock matrix elements between  $i$  and  $j$  NBO orbitals in a.u.

respective bond length and a lowering of the corresponding stretching wavenumber. The electron density (ED) is transferred from the  $n(C)$ ,  $n(N)$  to the anti-bonding  $\pi^*$  orbital of the C–N, C–O explaining both the elongation and the red shift[55]. The N–H, –C=O stretching modes can be used as a good probe for evaluating the bonding configuration around the corresponding atoms and the electronic distribution of the molecule. Hence the above structure is stabilized by these orbital interactions.

The NBO analysis also describes the bonding in terms of the natural hybrid orbital  $n2(F_{23})$ , which occupy a higher energy orbital  $-0.43558$ a.u.) with a considerable p-character (100.0%) and low occupation number (1.96205a.u.) and the other  $n1(F_{23})$  occupy a lower energy orbital  $(-1.10382)$  with p-character (21.61%) and

high occupation number (1.98877a.u.).Also  $n2(F_{24})$ , which occupy a higher energy orbital  $(-0.43640$ a.u.) with considerable p-character (99.99%) and low occupation number (1.96241a.u.) and the other  $n1(F_{24})$  occupy a lower energy orbital  $(-1.10464$ a.u.) with p-character (21.60%) and high occupation number (1.98882a.u.). Again  $n2(F_{25})$ , which occupy a higher energy orbital  $(-0.42919$ a.u.) with considerable p-character (99.73%) and low occupation number (1.96241a.u.) and the other  $n1(F_{25})$  occupy a lower energy orbital  $(-1.10506$ a.u.) with p-character (20.74%) and high occupation number (1.98904a.u.). Thus, a very close to pure p-type lone pair orbital participates in the electron donation to the  $\sigma^*(C-C)$  orbital for  $n(F) \rightarrow \sigma^*(C-C)$  interactions in the compound. The results are tabulated in Table 4.

**Table 4**  
NBO results showing the formation of Lewis and non-Lewis orbitals.

Bond (A–B)	ED/energy <sup>a</sup>	EDA (%)	EDB (%)	NBO	s (%)	p (%)
$\sigma C_1-N_6$	1.98361	39.03	60.97	0.6247(sp <sup>2.27</sup> )C	30.55	69.45
–	–0.86634	–	–	+0.7041(sp <sup>1.00</sup> )N	36.07	63.93
$\sigma C_1-N_6$	1.71948	42.38	57.62	0.6510(sp <sup>1.00</sup> )C	0.00	100.0
–	–0.34340	–	–	+0.7591(sp <sup>1.00</sup> )N	0.00	100.0
$\sigma N_3-C_4$	1.98230	60.51	39.49	0.7779(sp <sup>1.91</sup> )N	34.38	65.62
–	–0.85429	–	–	+0.6284(sp <sup>2.20</sup> )C	31.25	68.75
$\pi N_3-C_4$	1.69101	58.88	41.12	0.7673(sp <sup>1.00</sup> )N	0.00	100.0
–	–0.33309	–	–	+0.6413(sp <sup>1.00</sup> )C	0.00	100.0
$\sigma C_5-C_8$	1.96777	51.60	48.40	0.7183(sp <sup>2.08</sup> )C	32.50	67.50
–	–0.68758	–	–	0.6957(sp <sup>1.88</sup> )C	34.74	65.26
$\pi C_8-O_{19}$	1.97049	30.84	69.16	0.5553(sp <sup>1.00</sup> )C	0.00	100.0
–	–0.38216	–	–	+0.8316(sp <sup>1.00</sup> )O	0.00	100.0
$\pi C_9-C_{10}$	1.60844	49.40	50.60	0.7029(sp <sup>1.00</sup> )C	0.00	100.0
–	–0.27101	–	–	+0.7113(sp <sup>1.00</sup> )C	0.00	100.0
$\pi C_{10}-C_{11}$	1.97477	49.79	50.21	0.7057(sp <sup>1.81</sup> )C	35.64	64.36
–	–0.70744	–	–	+0.7086(sp <sup>1.79</sup> )C	35.79	64.21
$\pi C_{11}-C_{12}$	1.66648	43.86	56.14	0.6623(sp <sup>1.00</sup> )C	0.00	100.0
–	–0.27614	–	–	+0.7492(sp <sup>1.00</sup> )C	0.00	100.0
$\sigma N_{18}-H_{20}$	1.98027	73.19	26.81	0.8555(sp <sup>2.61</sup> )N	27.70	72.30
–	–0.67744	–	–	+0.5178(sp <sup>1.95</sup> )H	100.0	0.00
$\sigma C_{22}-F_{23}$	1.98887	26.65	73.35	0.5163(sp <sup>3.83</sup> )C	20.71	79.29
–	–0.95314	–	–	+0.8564(sp <sup>3.63</sup> )F	21.59	78.41
$\sigma C_{23}-F_{24}$	1.98890	26.60	73.40	0.5157(sp <sup>3.85</sup> )C	20.61	79.39
–	–0.95198	–	–	+0.8568(sp <sup>3.64</sup> )F	21.57	78.43
$n1C_2$	0.89702	–	–	sp <sup>1.00</sup>	0.00	100.0
–	–0.14796	–	–	–	–	–
$n1N_3$	1.92760	–	–	sp <sup>2.42</sup>	29.22	70.78
–	–0.35960	–	–	–	–	–
$n1C_5$	0.98894	–	–	sp <sup>1.00</sup>	0.00	100.0
–	–0.16247	–	–	–	–	–
$n1N_6$	1.91986	–	–	sp <sup>2.46</sup>	28.94	71.06
–	–0.38400	–	–	–	–	–
$n1N_{18}$	1.63050	–	–	sp <sup>1.00</sup>	0.00	100.0
–	–0.28655	–	–	–	–	–
$n1O_{19}$	1.97563	–	–	sp <sup>0.55</sup>	64.72	35.28
–	–0.70584	–	–	–	–	–
$n2O_{19}$	1.88860	–	–	sp <sup>1.00</sup>	0.00	100.0
–	–0.27747	–	–	–	–	–
$n1F_{23}$	1.98877	–	–	sp <sup>0.28</sup>	78.39	21.61
–	–1.10382	–	–	–	–	–
$n2F_{23}$	1.96205	–	–	sp <sup>1.00</sup>	0.00	100.0
–	–0.43558	–	–	–	–	–
$n3F_{23}$	1.94289	–	–	sp <sup>99.99</sup>	0.02	99.98
–	–0.43496	–	–	–	–	–
$n1F_{24}$	1.98882	–	–	sp <sup>0.28</sup>	78.40	21.60
–	–1.10464	–	–	–	–	–
$n2F_{24}$	1.96241	–	–	sp <sup>99.99</sup>	0.01	99.99
–	–0.43640	–	–	–	–	–
$n3F_{24}$	1.94369	–	–	sp <sup>99.99</sup>	0.02	99.98
–	–0.43561	–	–	–	–	–
$n1F_{25}$	1.98904	–	–	sp <sup>0.26</sup>	79.26	20.74
–	–1.10506	–	–	–	–	–
$n2F_{25}$	1.96241	–	–	sp <sup>99.99</sup>	0.27	99.73
–	–0.42919	–	–	–	–	–
$n3F_{25}$	1.94334	–	–	sp <sup>1.00</sup>	0.00	100.0
–	–0.42681	–	–	–	–	–

<sup>a</sup> ED/energy is expressed in a.u.

### Frontier molecular orbitals

The analysis of the wavefunction indicates that the electron absorption corresponds to a transition from the ground to the first excited state and is mainly described by one electron excitation from the HOMO to LUMO. Both the HOMO and the LUMO are the main orbital taking part in chemical reaction. The HOMO energy characterizes the capability of electron giving; LUMO characterizes the capability of electron accepting [56]. The frontier orbital gap helps to characterize the chemical reactivity, optical polarizability and chemical hardness–softness of a molecule [57]. Surfaces for the frontier orbitals were drawn to understand the bonding scheme of the title compound. Two important molecular orbitals (MO) were examined for the title compound, the highest occupied molecular orbital (HOMO) and the lowest unoccupied molecular orbital (LUMO) which are given in Figs. 4 and 5. The calculated HOMO and LUMO energies are  $-8.486$  and  $-5.21$  eV. The chemical hardness and softness of a molecule is a good indication of the chemical stability of the molecule. From the HOMO–LUMO energy gap, one can find whether the molecule is hard or soft. The molecules having large energy gap are known as hard and molecules having a small energy gap are known as soft molecules. The soft molecules are more polarizable than the hard ones because they need small energy to excitation. The hardness value of a molecule can be determined as  $\eta = (-\text{HOMO} + \text{LUMO})/2$  [56]. The value of  $\eta$  of the title molecule is  $1.638$  eV. Hence we conclude that the title compound belongs to hard material.

### PES scan study

A detailed potential energy surface (PES) scan on dihedral angle  $\text{C}_5\text{—C}_8\text{—N}_{18}\text{—H}_{20}$  have been performed at B3LYP/SDD level to reveal the possible conformations of the title compound. The PES scan was carried out by minimizing the potential energy in all geometrical parameters by changing the torsion angle at every  $20^\circ$  from  $-180^\circ$  to  $+180^\circ$  rotation around the bond. The result obtained

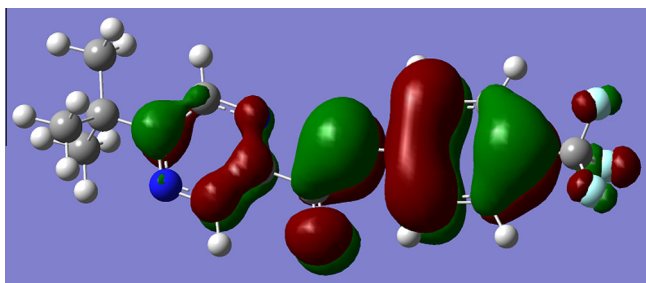


Fig. 4. HOMO plot of 5-tert-Butyl-N-(4-trifluoromethylphenyl)pyrazine-2-carboxamide.

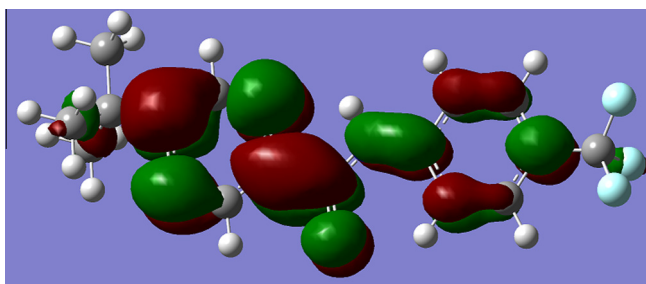


Fig. 5. LUMO plot of 5-tert-Butyl-N-(4-trifluoromethylphenyl)pyrazine-2-carboxamide.

in PES scan study is provided as Supplementary Material (Fig. S1). The minimum energy was obtained at  $0.0^\circ$  in the potential energy curve of energy  $-1145.4$  Hartree and above and below this torsion angle, the energy rises.

### Conclusion

The FT-IR and FT-Raman spectra of 5-tert-Butyl-N-(4-trifluoromethylphenyl)pyrazine-2-carboxamide were studied. The molecular geometry and wavenumbers were calculated using DFT methods and the optimized geometrical parameters (SDD) are in agreement with that of similar derivatives. The small differences between experimental and calculated vibrational modes are observed. This is due to the fact that experimental results belong to solid phase and theoretical calculations belong to gaseous phase. The calculated first hyperpolarizability is high and the title compound is an attractive object for future studies of non linear optics. The stability of the molecule arising from hyper-conjugative interaction and charge delocalization has been analyzed using NBO analysis. From the NBO analysis it is evident that the increased electron density at the nitrogen, carbon atoms leads to the elongation of respective bond length and a lowering of the corresponding stretching wavenumber.

### Acknowledgment

Hema Tresa Varghese would like to thank University Grants Commission, India for a research grant.

### Appendix A. Supplementary material

Supplementary data associated with this article can be found, in the online version, at <http://dx.doi.org/10.1016/j.saa.2013.04.101>.

### References

- [1] H. Endredi, F. Billes, F.S. Holly, J. Mol. Struct. Theochem. 633 (2003) 73–82.
- [2] M.C. Raviglione, C. Dye, S. Schmidt, A. Kochi, Lancet 350 (1997) 624–629.
- [3] S. Houston, A. Fanning, Drugs 48 (1996) 689–708.
- [4] M. Dolezal, Chem. Listy. 100 (2006) 959–966.
- [5] R.J. Speirs, J.T. Welch, M.H. Cynamon, Antimicrob. Agents Chemother. 39 (1995) 1269–1271.
- [6] C. Ngo, O. Zimhony, W.J. Chung, H. Sayahi, W.R. Jacobs Jr., J.T. Welch, Antimicrob. Agents Chemother. 51 (2007) 2430–2435.
- [7] A. Somoskovi, M.M. Wade, Z. Sun, Y. Zhang, J. Antimicrob. Chemother. 53 (2004) 192–196.
- [8] D.A. Mitchison, Natur. Med. 2 (1996) 635–636.
- [9] M.H. Cynamon, S.P. Klemens, T.S. Chou, R.H. Gimi, J.T. Welch, J. Med. Chem. 35 (1992) 1212–1215.
- [10] K.E. Bergmann, M.H. Cynamon, J.T. Welch, J. Med. Chem. 39 (1996) 3394–3400.
- [11] Y. Zhang, M.M. Wade, A. Scorpio, H. Zhang, Z. Sun, J. Antimicrob. Chemother. 52 (2003) 790–795.
- [12] A. Pawluko, I. Natkaniec, Z. Malarski, J. Leciejewicz, J. Mol. Struct. 516 (2000) 7–14.
- [13] F. Billes, H. Mikosch, S. Holly, J. Mol. Struct. Theochem. 423 (1998) 225–234.
- [14] K. Kralova, F. Sersen, M. Miletin, M. Dolezal, Chem. Pap. 56 (2002) 214–217.
- [15] K. Kralova, E. Masarovicova, F. Sersen, I. Ondrejovicova, Chem. Pap. 62 (2008) 358–363.
- [16] M. Dolezal, J. Hartl, M. Miletin, M. Machacek, K. Kralova, Chem. Pap. 53 (1999) 126–128.
- [17] M. Dolezal, J. Zitko, D. Kesetovicova, J. Kunes, M. Svobodova, Molecules 14 (2009) 4180–4189.
- [18] M.J. Frisch, G.W. Trucks, H.B. Schlegel, G.E. Scuseria, M.A. Robb, J.R. Cheeseman, G. Scalmani, V. Barone, B. Mennucci, G.A. Petersson, H. Nakatsuji, M. Caricato, X. Li, H.P. Hratchian, A.F. Izmaylov, J. Bloino, G. Zheng, J.L. Sonnenberg, M. Hada, M. Ehara, K. Toyota, R. Fukuda, J. Hasegawa, M. Ishida, T. Nakajima, Y. Honda, O. Kitao, H. Nakai, T. Vreven, J.A. Montgomery, Jr., J.E. Peralta, F. Ogliaro, M. Bearpark, J.J. Heyd, E. Brothers, K.N. Kudin, V.N. Staroverov, T. Keith, R. Kobayashi, J. Normand, K. Raghavachari, A. Rendell, J.C. Burant, S.S. Iyengar, J. Tomasi, M. Cossi, N. Rega, J.M. Millam, M. Klene, J.E. Knox, J.B. Cross, V. Bakken, C. Adamo, J. Jaramillo, R. Gomperts, R.E. Stratmann, O. Yazyev, A.J. Austin, R. Cammi, C. Pomelli, J.W. Ochterski, R.L. Martin, K. Morokuma, V.G. Zakrzewski, G.A. Voth, P. Salvador, J.J. Dannenberg, S. Dapprich, A.D. Daniels, O. Farkas, J.B.

- Foresman, J.V. Ortiz, J. Cioslowski, D.J. Fox, Gaussian 09, Revision B.01, Gaussian, Inc., Wallingford CT, 2010.
- [19] P.J. Hay, W.R. Wadt, *J. Chem. Phys.* 82 (1985) 270–283.
- [20] J.Y. Zhao, Y. Zhang, L.G. Zhu, *J. Mol. Struct. Theochem.* 671 (2004) 179–187.
- [21] J.B. Foresman, in: E. Frisch (Ed.), *Exploring Chemistry with Electronic Structure Methods: A Guide to using Gaussian*, Pittsburg, PA, 1996.
- [22] R. Dennington, T. Keith, J. Millam, Gaussview, Version 5, Semichem Inc., Shawnee Mission, KS, 2009.
- [23] J.M.L. Martin, C. Van Alsenoy, GAR2PED, A Program to obtain a Potential Energy Distribution from a Gaussian Archive Record, University of Antwerp, Belgium, 2007.
- [24] N.P.G. Roeges, *A Guide to the Complete Interpretation of Infrared Spectra of Organic Structures*, Wiley, New York, 1994.
- [25] A. Spire, M. Barthes, H. Kellouai, G. DeNunzio, *Physics D* 137 (2000) 392–396.
- [26] L.J. Bellamy, *The Infrared Spectrum of Complex Molecules*, third ed., Chapman and Hall, London, 1975.
- [27] N.B. Colthup, L.H. Daly, S.E. Wiberly, *Introduction to Infrared and Raman spectroscopy*, third ed., Academic Press, Boston, 1990.
- [28] Y.S. Mary, H.T. Varghese, C.Y. Panicker, M. Dolezal, *Spectrochim. Acta* 71 (2008) 725–730.
- [29] S. Kundoo, A.N. Banerjee, P. Saha, K.K. Chattopadhyay, *Mater. Lett.* 57 (2003) 2193–2197.
- [30] A.G. Iriarte, E.H. Cutin, M.F. Erben, S.E. Ulic, J.L. Jios, C.O.D. Vedova, *Vib. Spectrosc.* 46 (2008) 107–114.
- [31] V. Schettino, G. Sbrana, R. Righini, *Chem. Phys. Lett.* 13 (1972) 284–285.
- [32] J.F. Arenas, J.T.L. Navarrete, J.C. Otero, J.I. Marcos, A. Cardenete, *J. Chem. Soc. Faraday Trans. 2* (81) (1985) 405–415.
- [33] G. Varsanyi, *Assignments of Vibrational Spectra of Seven Hundred Benzene derivatives*, Wiley, New York, 1974.
- [34] Y.S. Mary, H.T. Varghese, C.Y. Panicker, T. Ertan, I. Yildiz, O. Temiz-Arpaci, *Spectrochim. Acta* 71 (2008) 566–571.
- [35] A.R. Ambujakshan, V.S. Madhavan, H.T. Varghese, C.Y. Panicker, O. Temiz-Arpaci, B. Tekiner-Gulbas, I. Yildiz, *Spectrochim. Acta* 69 (2007) 782–788.
- [36] H. Ptasiwicz-Bak, J. Leciejewicz, *Polish. J. Chem.* 71 (1997) 1350–1358.
- [37] B.J.M. Bormans, G. De-With, F. Mijlhoff, *J. Mol. Struct.* 42 (1997) 121–128.
- [38] H. Endredi, F. Billes, G. Keresztury, *J. Mol. Struct. Theochem.* 677 (2004) 211–225.
- [39] V. Chis, A. Pirnau, T. Jurca, M. Vasilescu, S. Simon, O. Cozar, L. David, *Chem. Phys.* 316 (2005) 153–163.
- [40] W. He, G. Zhou, J. Li, A. Tian, *J. Mol. Struct. Theochem.* 668 (2004) 201–208.
- [41] S.M. Bakalova, A.G. Santos, I. Timcheva, J. Kaneti, I.L. Filipova, G.M. Dobrikov, V.D. Dimitrov, *J. Mol. Struct. Theochem.* 710 (2004) 229–234.
- [42] M. Barthes, G. DeNunzio, G. Ribet, *Synth. Meter.* 76 (1996) 337–340.
- [43] P. Anbarasu, M. Arivazhagan, *Indian J. Pure Appl. Phys.* 49 (2011) 227–233.
- [44] V. Krishnakumar, R.J. Xavier, *Spectrochim. Acta* 61 (2005) 253–260.
- [45] J.C. Noveron, A.M. Arif, P.J. Stang, *Chem. Mater.* 15 (2003) 372–374.
- [46] H. Takeuchi, M. Sato, T. Tsuji, H. Takashima, T. Egawa, S. Konaka, *J. Mol. Struct.* 485–486 (1999) 175–181.
- [47] E.D. Stevens, *Acta Cryst.* 34B (1978) 544–551.
- [48] Q. Gao, G.A. Jeffrey, J.R. Ruble, R.K. McMullan, *Acta Cryst.* 47B (1991), pp. 742–645.
- [49] K. Tamagawa, T. Iijima, M. Kimura, *J. Mol. Struct.* 30 (1976) 243–253.
- [50] K.B. Borizenko, C.W. Bock, I. Hargitai, *J. Phys. Chem.* 100 (1996) 7426–7434.
- [51] D.A. Kleinman, *Phys. Rev.* 126 (1962) 1977–1979.
- [52] Y.P. Tian, W.T. Yu, C.Y. Zhao, M.H. Jiang, Z.G. Cai, H.K. Fun, *Polyhedron* 21 (2002) 1217–1222.
- [53] T. Joseph, H.T. Varghese, C.Y. Panicker, K. Viswanathan, N. Sundaraganesan, N. Subramanina, M. Dolezal, *Global J. Anal. Chem.* 3 (2012) 1–12.
- [54] E.D. Glendening, A.E. Reed, J.E. Carpenter, F. Weinhold, NBO Version 3.1, Gaussian Inc., Pittsburg, PA 2009.
- [55] J. Choo, S. Kim, H. Joo, Y. Kwon, *J. Mol. Struct. (Theochem.)* 587 (2002) 1–8.
- [56] K. Fukui, *Science* 218 (1982) 747–754.
- [57] B. Kosar, C. Albayrak, *Spectrochim. Acta* 78A (2011) 160–167.